Brain Research Bulletin 239 (2026) 111883

Contents lists available at ScienceDirect

Brain Research Bulletin

journal homepage: www.elsevier.com/locate/brainresbull

Research report

Exposure to a high-fat diet compromises gut health, behavior, and HPA axis function, with partial reversal when limited to adolescence

Alexandra Ott [a,*], Asude Zülal Gül [a], Ulrike Löber [b], Till Birkner [b], Elena Popova [b], Christine Winter [a], Ravit Hadar [a]

[a] Charité – Universitätsmedizin Berlin, corporate member of Freie Universität Berlin and Humboldt-Universität zu Berlin, Klinik für Psychiatrie und Psychotherapie, Forschung, AG Experimentelle Psychiatrie, Charitéplatz 1, Berlin 10117, Germany
[b] Max-Delbrück-Center for Molecular Medicine (MDC), Robert-Rössle-Str.10, Berlin 13125, Germany

ARTICLE INFO

Key Words:
Diet, High-Fat
Adolescent
Intergenerational Relations
Gastrointestinal Microbiome
HPA Axis

ABSTRACT

High-fat diet (HFD) consumption contributes to obesity, yet its impact on females of (pre)reproductive age and the effects of dietary modification after adolescence remain underexplored. This study examined how continuous HFD exposure or an adolescent switch from HFD to a standard diet (SD) shapes the gut microbiome, behavior, neurochemistry, metabolism, and key components of the hypothalamic–pituitary–adrenal (HPA) axis in female rats. Because HPA-axis alterations can occur across generations after HFD exposure, we examined reproductive-tissue HPA-axis components as potential mechanisms of transmission.

Females received SD, HFD, or HFD followed by SD after majority of adolescence (postnatal day 60). HFD exposure impaired HPA-axis regulation and switching to SD during adolescence did not prevent persistent dysfunction into adulthood. However, reproductive HPA-axis components remained unaltered. Diet also strongly influenced the microbiome: while HFD disrupted microbial composition in adolescence, switching to SD partially restored it by adulthood. Behavioral and metabolic effects, including increased adiposity and anxiety-like behavior, emerged only with prolonged HFD exposure. Brain neurotransmitter concentrations remained largely unaffected.

Overall, dietary history across adolescence and early adulthood shaped long-term HPA-axis function, microbiome composition, and behavioral outcomes. The absence of reproductive HPA-axis alterations suggests it is not a major mediator of maternal HFD-induced intergenerational effects. Persistent HPA-axis dysfunction despite dietary switching indicates limited reversibility, whereas the microbiome showed the greatest adaptive capacity. In contrast, lasting behavioral and metabolic consequences of HFD require continued exposure to adulthood.

1. Introduction

The World Health Organization (WHO) declared obesity an epidemic as early as 1997, acknowledging it as a major challenge for healthcare systems and attributing it to millions of deaths annually (Obesity WHOCo et al., 1998). Obesity is tightly associated with preventable maladies like diabetes and cardiovascular disease (Obesity WHOCo et al., 1998). However, it has also been linked to a variety of behavioral, biochemical, and, in recent years, microbiota alterations (Lafortuna et al., 2017). The consumption of high-fat diet (HFD) contributes to the obesity epidemic (Buckley, 2018) and is itself linked to changes in microbiome and cognitive impairments (Mabrok et al., 2024). The bidirectional link between gut health and cognitive function has recently gained significant attention in research on the "Brain-Gut Axis" (Shoubridge et al., 2022). Recent studies highlighted the importance of the Brain-Gut Axis, showing that HFD-induced microbiome changes affect serotonergic systems linked to depression and anxiety (de Noronha et al., 2024) and contribute to cognitive impairments (Mabrok et al., 2024). Human studies investigating the correlation between HFD and cognitive function are scarce, primarily focusing on elderly subjects and their dementia risk, yielding mixed results (Barnard et al., 2014). Nevertheless, several studies found that even a short period of HFD consumption by healthy young men is sufficient to induce a decline in attention and memory function (Edwards et al., 2011; Holloway et al., 2011). Similar outcomes, including manifestation of depression, were observed among elderly women (Roberts et al., 2012). Notably, studies

* Corresponding author.
E-mail address: Alexandra.ott@charite.de (A. Ott).

https://doi.org/10.1016/j.brainresbull.2026.111883
Received 16 October 2025; Received in revised form 17 March 2026; Accepted 7 April 2026
Available online 8 April 2026

frequently overlook young women of childbearing age, resulting in inadequate representation in research. Given that adolescence is recognized as a vulnerable phase in which environmental factors modulate neurobehavioral processes with lasting implications for cognitive outcomes (Spear, 2000), the tripling of childhood obesity prevalence since 1975 is of particular concern (Pulungan et al., 2024). Pre-clinical studies suggest that the timing of HFD exposition is critical for behavioral outcomes, as exposure during adolescence may lead to different results than exposure during adulthood (Ziemens et al., 2022). However, the potential lasting effects or reversibility of HFD limited to adolescence, including microbiome and behavioral changes, is a less frequently studied aspect and remains inconclusive in existing literature (Lloyd and Reyes, 2022; Boitard et al., 2016).

HFD can induce changes not only in directly exposed individuals but also in their offspring. It is widely accepted that maternal HFD exposure may lead to altered behavior and biochemistry in their offspring (Ziemens et al., 2022; Godfrey et al., 2017). Various approaches investigate the underlying mechanisms of this transmission. Among them, the HFD-induced alterations in the maternal microbiome appear to play a crucial role (Ratsika et al., 2024; Buffington et al., 2016), while another perspective highlights the significant influence of epigenetics and inflammation (Harmancıoğlu and Kabaran, 2023). Inflammation influences the Hypothalamic-Pituitary-Adrenal Axis (HPA axis) - a key pathway in stress response (Witchel and DeFranco, 2006). The HPA axis has been proposed as a pathway for the intergenerational transmission of stress, with evidence showing alterations in corticotropin-releasing hormone receptor 1 (CRF1) in the oocytes and ovaries of females exposed to pre-reproductive environmental stressors (Ott et al., 2025; Zaidan et al., 2013). Despite the limited examination of the HPA axis in HFD-exposed females, Rodriguez et al. pointed to an altered HPA axis function by identifying elevated Corticosterone (CORT) levels as the leading stress marker in rodents in HFD-exposed pregnant dams and linking this to the altered behavior of their offspring (Rodriguez et al., 2012). However, a pre-reproductive assessment of the HPA axis, including the reproductive system, in HFD-exposed females, as well as the potentially reversible effects on future generations and exposed individuals, awaits investigation. This study was therefore designed to explore the impact and potential reversibility of HFD on female rats during both adolescence and adulthood.

By exclusively focusing on female rats, this pre-clinical study takes into account the underrepresentation of childbearing-aged female subjects and the understudied influence of diet on potential future generations. The impact of HFD on individual health has been primarily studied on male subjects. Hence, this study aims to examine stress-axis, cognition, and gut health in females. Furthermore, by examining the oocytes, this study provides insight into potential offspring without actual reproduction, while controlling environmental factors.

2. Methods

2.1. Animals

Thirty female Sprague-Dawley rats, aged PND 21 (Janvier, France), were housed in groups of five, enriched with polycarbonate huts, cellulose paper, and chew sticks. The rats were housed in a temperature- and humidity-controlled environment with a 12-hour light-dark cycle, where lights turned off at 6 pm. They had access to water and food ad libitum. All behavioral tests were performed during the animals' active phase (dark cycle) and in accordance with European regulations (2013/63/EU), the German Animal Welfare Act (last revised in 2014), and with approval from the local animal welfare authority (LaGeSo Berlin).

2.2. Procedure

To investigate the effect of diet during adolescence, young female rats received a high-fat diet (HFD (60% Fat), ssniff #EF D12492, Soest, Germany) ad libitum during PND 21–60, correlating with rodents' adolescent stage (Spear, 2000). Subsequently, they were transitioned to a standard diet ((SD: 11% Fat), Altromin #1324, Lage, Germany). Control groups remained on either HFD or SD throughout the experiment.

Study design is shown in Fig. 1. Briefly, **behavioral tests** (T-Maze Alternation, Elevated Plus Maze (EPM), Novel Object Recognition (NOR) and Pre-Pulse Inhibition (PPI)), blood and stool collection were performed before the transition to SD (at PND 60) and at the end of the experiment, as the animals reached adulthood (at PND 90). **Fecal microbiome** was analyzed via 16S rRNA gene analysis. **Intestinal Permeability** was evaluated ex vivo after completing behavioral tests after PND 90. Serum was analyzed for metabolic markers and **CORT**. For further evaluation of HPA axis and the potential impact of the diet on future generations, animals were superovulated, and oocytes and ovaries **CRF1-Expression** analyzed using RT-PCR were examined. Furthermore, **neurochemistry** was assessed in amygdala, frontal cortex, and hippocampus post mortem.

2.2.1. Behavioral tests

Behavioral tests (T-Maze Alternation, Elevated Plus Maze (EPM), Novel Object Recognition (NOR) and Pre Pulse Inhibition (PPI)) were conducted at PND 56–59 and PND 86–89 in the following order:

2.2.1.1. T-Maze alternation. Cognitive function was assessed using a spontaneous alternation task in a T-Maze paradigm, as described by Deacon et al (Deacon and Rawlins, 2006; Cifre et al., 2018). This paradigm evaluates short-term memory and flexibility in a free trial approach by measuring the capacity to recall the arm the animal had previously chosen and select a different arm when reintroduced to the T-maze.

Each animal was placed at the start area of the T-Maze and allowed to select an arm. After choosing one arm, it was restricted to that arm for 30 s. This procedure was repeated 5 times. A score of 1 was assigned when the animal opted for an arm different from its first choice, while a score of 0 was recorded if it selected the same arm. These scores were used to calculate the corrected percentage of success. In parallel, latency (the time it took for the animal to choose an arm) was recorded to identify potential cognitive dysfunction that might affect the decision-making process.

2.2.1.2. EPM. The Elevated Plus Maze Test was used to evaluate anxiety. The maze consists of two closed and two open arms of equal length. The animals were placed in the center of the maze, facing one of the enclosed arms. Behavior was recorded for 10 min and analyzed using Ethovision (EthoVision XT 7.0, Noldus Information Technology, Wageningen, The Netherlands). Arm entry is defined by the central point of the animal crossing into one of the arms. Frequency and duration of entries were analyzed to quantify anxiety levels. Additionally, the total distance moved was measured to detect potential locomotor impairments.

2.2.1.3. NOR. Novel Object Recognition Test (NOR) is a widely utilized method to assess memory function of rodents (Antunes and Biala, 2012). Rodents tend to display more interest in novel objects compared to familiar ones (Antunes and Biala, 2012; Ennaceur and Delacour, 1988).

Animals were habituated to the testing room and subsequently introduced to an open field arena, where they were allowed to explore two identical objects placed in opposite corners for five minutes. After a ninety-minute break, the animals were reintroduced to the field for another five minutes, with one of the familiar objects being replaced with a novel one. The behavior was filmed and analyzed using Ethovision. Interaction time with both the novel and familiar object was quantified, with interaction defined as the animal's nose-point being within a distance of less than 2 cm from the object (Leo et al., 2019).

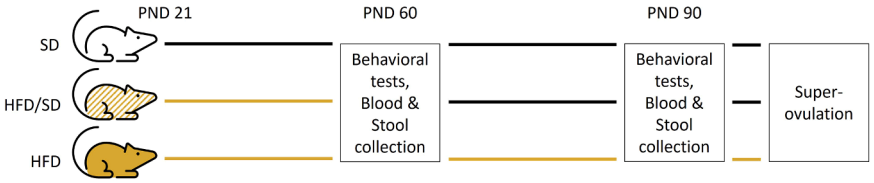

Fig. 1. Study Design. *Fill color indicates HFD exposure; striped patterns denote diet switch.*

Furthermore, total distance moved was analyzed to identify locomotor impairments (Leo et al., 2019). Novel object recognition was measured by calculating the discrimination index ((time spent with novel object - time spent with familiar object)/ exploration time objects). Induced preference was assessed by computing the discrimination index of training phase. Values exceeding zero were interpreted as a preference for novelty, indicating the presence of recognition memory, while values under 0 displayed a preference for the familiar object (Antunes and Biala, 2012).

2.2.1.4. PPI. Pre-pulse inhibition (PPI) of the Acoustic Startle Response (ASR) was measured in a sound-attenuated chamber with a speaker (Startle response system, TSE, Germany). The animals were restrained in a wire-mesh cage that was mounted on a piezoelectric platform to measure the ASR (Hadar et al., 2015). After a five-minute habituation phase, animals were exposed to the following trials in pseudorandom order: pulse alone (100 dB), 20 ms; control (no stimulus); Pre-Pulse alone (69 dB, 73 dB, or 81 dB); Pre-Pulse followed by pulse with an interstimulus interval of 100 ms. A total of 10 presentations of each type were delivered, with inter-trial periods lasting 20–30 s. The background intensity was maintained at 60 dB (white noise) throughout the experiment. The average PPI across the three Pre-Pulse intensities was calculated: PPI was defined as: PPI(X) = (Pulse – Pre-Pulse X)/(Pulse), where X = 69 dB, 73 dB, or 81 dB (Mattei et al., 2014).

2.2.2. HPA axis assessment

2.2.2.1. CORT. One day after completing the behavioral tests (at PND 60 and PND 90), blood was collected from the tail vein under short isoflurane anesthesia. To evaluate the circadian rhythm of CORT, serum samples collected during the active phase (at PND 60 and PND 90) were compared with trunk blood obtained several days later during sacrifice in the inactive phase.

Samples were allowed to sit for one hour and were centrifuged for 25 min at 10 G at 4 °C. Serum and stool were stored at −80 °C until further processing. CORT serum levels were quantified using ELISA (Enzyme-Linked Immunosorbent Assay), with sample processing following the manufacturer's protocol (#RE52211, Tecan).

2.2.2.2. CRF1 expression. After Completing behavioral tests at PND 90, animals underwent a 2-day ovulation induction. Mature oocytes and ovaries were collected and CRF1-Expression analyzed using RT-PCR.

2.2.2.3. Superovulation induction. Ovulation was induced as previously described (Zaidan et al., 2013). Dams received an i.p. injection with 40 IU PMSG (pregnant mare's serum gonadotropin) in 300 µL of PBS (Pregmagon, Ceva, Germany), followed by 40 IU hCG (human chorionic gonadotropin) (Ovogest, MSD, Germany) in 300 µL PBS 44–48 h later. After 24 h, the animals were put under deep Isoflurane anesthesia and were decapitated. Oviducts were extracted and placed in M2 Medium (#M7167, Sigma Aldrich). Along with the oviducts, brains, ovaries, and trunk blood were collected, snap-frozen on dry ice, and stored at −80 °C until further processing.

2.2.2.4. Oocyte isolation. Oocytes were released from the oviducts. Cumulus cells were removed by incubating them with hyaluronidase enzyme (200 IU/mL, Sigma Aldrich, #H4272) (Choi and He, 2013). Subsequently, the oocytes were counted and washed with PBS. RNA isolation was performed immediately thereafter.

2.2.2.5. Gene expression analysis by RT-PCR. RNA isolation was conducted using Quiazol Lysis Reagent (#79306, Qiagen) in accordance with the manufacturer's instructions. The resulting RNA from the oocyte samples was dissolved in 10 µL of water, while RNA from ovaries was dissolved in 50 µL of water. The quantity and quality of the RNA were assessed using a Nanodrop 2000 (Applied Biosystems). Only samples with a 260:280 nm absorbance ratio of at least 1.7 for oocytes and 2.0 for ovaries were included in the subsequent steps. Following the manufacturer's protocol, reverse transcription was carried out using the High-Capacity cDNA Reverse Transcription kit (#4387406, ThermoFisher).

For qPCR, cDNA was amplified in the duplicate reaction of 20 µL each: 10 µL Powerup SYBR green Mastermix (#A25742, ThermoFischer), each 1 µL forward/reverse Primer (10 mM), 8 µL cDNA (Ovaries RNA was diluted 1:3).

qPCR was performed using a StepOne RT-PCR system (Eppendorf, Mastercycler ep realplex 2) with the following PCR conditions: 50 °C for 2 min, 95 °C for 2 min, followed by 40 cycles (95 °C for 15 s, 55 °C for 15 s, 72 °C for 1 min). Subsequently, a melting curve analysis (95 °C for 15 s, 60 °C for 1 min, 95 °C for 15 s) was performed.

Zaidan et al (Zaidan et al., 2013). previously established the primer sequences synthesized by TIB MOLBIOL Syntheselabor GmbH (Berlin, Germany).

Gene	Forward primer	Reverse primer
CRF1	5′ACGAAGAGAAGAAGAGCAAAGTACA3′	5′AGATGCAGTGACCCAGGTAGTTG3′
HPRT	5′CGCCAGCTTCCTCCTCAG3′	5′ATAACCTGGTTCATCATCACTAATCAC3′

Primer suitability was assessed through standard curve analysis, melting curve analysis, and gel electrophoresis. Primer dimers were detected by amplification without the addition of cDNA. To calculate the fold change, the ΔΔCt method was used (Livak and Schmittgen, 2001). Ct values for the target gene CRF1 were normalized to the housekeeping gene HPRT (hypoxanthine phosphoribosyl transferase). The fold change was calculated as $2^{-\Delta\Delta Ct}$ relative to the average of control samples. The values were log-transformed.

2.2.3. Metabolic markers

Metabolic markers were analyzed photometrically in an accredited commercial laboratory, including glucose, fructosamine, HDL, LDL, and triglycerides in serum samples.

2.2.4. Gut assessment

2.2.4.1. Fecal microbiome. Fecal samples were collected during blood collecting (at PND 60 and PND 90). Samples were snap-frozen on dry ice and stored at −80°C until further processing.

Stool preparation and 16S rRNA gene analysis were performed by Institut für Molekularbiologie Kiel, as described earlier (Troci et al., 2022). Briefly, fecal samples were transferred to Power Bead Pro tubes (QIAGEN GmbH, Germany) filled with 1 mL InhibitEx buffer and bead-beat for 45 s at 60 Hz using a SpeedMill PLUS Homogenizer (Analytik Jena, Jena, Germany). Afterward, samples were incubated at 95°C for 5 min, centrifuged at 10,000 rpm for 1 min, and 200 µl supernatant was used for automatic DNA extraction on Qiacubes using the QIAamp Fast DNA Stool Mini Protocol for Isolation of DNA from Stool for Pathogen Detection' with elution in 200 µl ATE buffer (QIAGEN GmbH, Germany). The V3-V4 variable regions of the 16S rRNA gene were amplified in a one-step PCR using the primer pair 341F-806R (dual-barcoding approach (Kozich et al., 2013); primer sequences: 5'-CCTACGGGAGGCAGCAG-30 and 5'-GGACTACHVGGGTWTCTAAT-30). After verification of the presence of PCR products by gel electrophoresis, normalization (Sequal Prep Normalization Plate Kit; Thermo Fisher Scientific, Waltham, USA) and equimolar pooling were performed. Sequencing was conducted on the MiSeq platform (MiSeq; Illumina, San Diego, USA) with v3 chemistry.

Sequences derived from stool samples were processed using LotuS2 (v2.25) (Özkurt et al., 2022; Bedarf et al., 2021; Li, 2018; Rognes et al., 2016). Poisson binomial model-based read filtering was applied (Puente-Sánchez et al., 2016). OTU clustering (UPARSE) (Edgar, 2013) was based on sequence similarity of 97%, while SILVA 138 (Yilmaz et al., 2014) was used as a database for a taxonomic assignment using a Lambda (Hauswedell et al., 2014) taxonomic similarity search. Normalization was performed using the Rarefaction Tool Kit (RTK 0.93.1) with default settings (Saary et al., 2017). Alpha and beta diversity at the OTU level were calculated using the Vegan package in R (Oksanen et al., 2025). Bray-Curtis dissimilarity was calculated using the adonis2 function from the vegan package. Subsequently, the pairwiseAdonis package was used to perform pairwise comparisons (Martinez Arbizu, 2017). Differential abundance analyses were conducted using metadeconfoundR (version 1.0.2) with default settings (Forslund et al., 2021; Birkner, 2024). Initially, associations between rarefied bacterial read counts and diet were assessed using rank-based Wilcoxon tests with FDR adjustment. Cliff's Delta was used to estimate effect sizes. To account for repeated measures, the randomVar parameter was applied (Schoeler et al., 2023). Genus-level visualizations and heat tree plots were generated using the metacoder package (Foster et al., 2017).

2.2.4.2. Ex vivo intestinal permeability measurement. Following a deep Isoflurane anesthesia, the animals were decapitated, and an abdominal cavity was opened. Gut permeability was assessed following the methods described by Mateer et al (Lippai et al., 2021; Mateer et al., 2016). Briefly, a 7 cm-long segment of the small intestine (located approximately 30 cm from the stomach) was flushed with PBS (#10010023, ThermoFischer) and fashioned into sacks by securely knotting the ends. These sacks were filled with 1 mL of FITC-conjugated Dextran 3–5 kDa (1 mg/mL) (#FD4, SigmaAldrich) diluted in pre-oxygenated and preheated medium (FluoroBrite DMEM, #A1896701, ThermoFischer). These dextran-loaded sacks were submerged in 40 mL of the same medium at 37 °C. Dextran permeation was assessed at 30-minute intervals over a period of two hours. Afterward, the sacks were opened to release the remaining dextran, representing 100% potential release. The fluorescence intensities of medium samples were measured at λexc: 485 nm, λem: 535 nm in a Microplate Reader (Spectra Max iD3, SoftMax Pro 7.1, Molecular Devices, USA). Data points were normalized relative to the 100% potential release, and the area under the curve was calculated.

2.2.5. Neurochemistry

For neurochemical analyses, the amygdala (AMY), frontal cortex (FC), and hippocampus (HIP) were dissected and homogenized on ice in 0.1 N perchloric acid (HPLC grade; Merck, Germany). Amino acid and catecholamine quantification was performed as previously described (Winter et al., 2009). For amino acid analysis, homogenate aliquots were mixed in a 1:1 ratio with o-phthalaldehyde diluent (Pickering Laboratories, USA). Aspartate, glutamine, glutamate, GABA, and taurine were measured following pre-column derivatization with o-phthalaldehyde and 2-mercaptoethanol (3:2), neutralized with 0.5 mM acetic acid (5:2), and separated using HPLC (AppliChrom TriKala C18, 75 × 3 mm) at a flow rate of 0.7 mL/min and a column temperature of 25 °C. A linear acetonitrile gradient (12–28%) in sodium acetate buffer (pH 5.7) was applied. Fluorescence detection was performed at 450 nm (emission) following excitation at 330 nm using a fluorescence detector (RF-10AXL, Shimadzu, Japan). Catecholamines including noradrenaline (NA), dopamine (DA), serotonin (5-HT), tryptophan (Trp), and their metabolites (DOPAC, HVA, and 5-HIAA) were quantified using HPLC with electrochemical detection (EC6000, Recipe Chemicals + Instruments GmbH, Germany) on a Prontosil 120–5-C18-SH column (150 × 3 mm; Bischoff Analysentechnik, Germany). Neurotransmitter concentrations were determined by peak integration using LabSolutions software (version 5.97, Shimadzu) and normalized to protein content. Protein concentration was assessed using the Pierce™ Coomassie (Bradford) Protein Assay Kit (Thermo Fisher Scientific, USA) according to the manufacturer's instructions.

2.3. Statistics

Analysis was conducted in RStudio (version 2023.09.1 +494) with R (version 4.4.2), utilizing the tidyverse package for data processing and visualization (Wickham et al., 2019).

Repeated measures analyses of variance were performed using linear mixed-effects models (LMM) via the lme4 package in R (Bates et al., 2015). The models included Age and Diet as fixed effects, with random intercepts for subjects (ID) to account for repeated measures. Model significance was assessed using Type III ANOVA performed on the fitted model using the lmerTest package (LMM ANOVA) (Kuznetsova et al., 2017). We conducted pairwise comparisons between groups at each time point to interpret significant interactions by post hoc Tukey test with emmeans package (Lenth, 2024). Suppose LMM ANOVA revealed a significant age effect; subsequently, one-way ANOVAs were conducted separately at each time point by fitting linear regression models. Homogeneity of variance was assessed using Levene's test. Post-mortem tests (gut permeability and ovary analysis) without age component were analyzed using one-way ANOVA followed by multiple comparisons (Tukey method). Statistical significance was established at a p-value of $p \leq 0.05$. The removal of outliers, where applicable, was performed using the 1.5 IQR method. To ensure internal consistency of the dataset, when a value was identified as an outlier at one time point, the corresponding paired measurement from the same subject at the alternate time point was also excluded from analysis.

3. Results

3.1. Weight

Weight development across the groups: LMM ANOVA (diet, age; n = 10 per group) revealed a main effect of diet ($F_{[2,\ 72]} = 18.12$,

p < 0.0001) and age *($F_{[2, 72]} = 34.34$, $p < 0.0001$)*. No significant weight differences were observed before the diet switch (PND 58). Subsequent to the switch (PND 65), HFD/SD animals significantly increased in weight compared to SD *(Diet: $F_{[2, 27]} = 4.39$, $p = 0.02$; Levene's test = 0.51; HFD/SD and SD ($p = 0.02$))*. On the final measurement day (PND 86), animals that continued with HFD weighed significantly more than SD (Diet: $F_{[2, 27]} = 3.47$, p = 0.046; *Levene's test = 0.5; HFD and SD ($p = 0.04$))*. Although not statistically significant, the weight of animals that switched to SD after HFD exposure during adolescence appears to be higher than that of animals on lifelong SD (see Fig. S1 in Supplementary).

3.2. Behavior

While no significant differences in **NOR** or **T-Maze Alternation** tests were detected, analysis of PPI and EPM revealed a significant impact of age, highlighting that age, and thus neurodevelopment, has a substantial impact on these behaviors. LMM ANOVA (age, diet), n = 7–9 per group, yielded significant differences in **PPI** results between adolescence and adulthood, with adult animals consistently displaying heightened inhibition following all presented Pre-Pulses, *Main effect for Age*: 69 dB *($F_{[1, 20]} = 35.48$, $p < 0.001$)*, 73 dB *($F_{[1, 40]} = 17.49$, $p = 0.0002$)*, 81 dB *($F_{[1, 20]} = 17.26$, $p = 0.0005$)*. Age-separate analysis did not yield any diet effect. The LMM ANOVA (age, diet), n = 10 per group, revealed age-dependent differences in the time spent across the different **EPM** arms: Adult animals spent less time in closed arm *($F_{[1, 54]} = 14$, $p = 0.0004$)* and more time in open arms *($F_{[1, 48]} = 4.88$, $p = 0.03$)* compared to their adolescent counterparts, indicating less anxious behavior in adulthood. Additionally, LMM ANOVA (age, diet) of the frequency of arm entrances showed age-dependency: *Main Effect for age:* frequency closed arm *($F_{[1, 45]} = 86.54$, $p < 0.001$)*, frequency open arm *($F_{[1, 48]} = 18.76$, $p < 0.001$)*, frequency center *($F_{[1, 45]} = 9.40$, $p = 0.004$)*. Due to the main effect of age, age-separated analysis was performed. ANOVA (diet) of frequency of closed arm, Levene's Test: p = 0.23, revealed a *main effect for diet ($F_{[2, 27]} = 6.14$, $p = 0.01$)*, showing that adult animals on a lifelong HFD displayed a significant preference for closed arms, entering this area more often compared to the other groups: significant post-hoc comparisons: *HFD* compared to *SD ($p = 0.02$)*, respectively to *HFD/SD ($p = 0.01$)* (Fig. 2). Distance moved was not significantly different across the groups.

3.3. Post-mortem

3.3.1. Metabolism

Analysis of serum metabolism parameters revealed no differences in **triglyceride** or **cholesterol** levels across groups or age groups. However, all other values decreased from adolescence to adulthood, as supported by LMM ANOVA (diet, age), n = 5 per group, revealing *main age effects* for: **glucose** *($F_{[1, 12]} = 5.03$, $p = 0.04$)*, **fructosamine** *($F_{[1, 12]} = 11.44$, $p = 0.01$)*, **HDL** *($F_{[1, 12]} = 30.67$, $p = 0.0001$)* and **LDL** *($F_{[1, 12]} = 55.21$, $p < 0.0001$)*. After outlier removal, the ANOVA (diet), n = 3–4, Levene's Test p = 0.73, of LDL levels, revealed a *main effect for diet ($F_{[2, 8]} = 5.41$, $p = 0.03$)*, post-hoc test showed increased LDL levels of *HFD* compared to *SD ($p = 0.04$)* at PND90 (Fig. S2).

3.3.2. HPA axis

CORT Analysis revealed an intact circadian rhythm among all groups, with physiologically higher CORT levels during the active phase in adulthood, supported by a LMM ANOVA (diet, time), n = 5–9, yielding a *main effect for time ($F_{[1, 19]} = 37.67$, $p = 6.72e\text{-}06$)*. After outlier removal, CORT values were calculated separately during the active and inactive phases. One-way ANOVA (diet), n = 4–7, Levene's test p = 0.23, of CORT levels during active period revealed a significant *main effect of diet ($F_{[2, 14]} = 11.30$, $p = 0.001$)* with significant higher CORT levels in both *HFD ($p = 0.001$)* as well as *HFD/SD ($p = 0.04$)* when compared to *SD* (Fig. 3A). While CORT levels did not differ between the groups at adolescence, LMM ANOVA (diet, age), n = 4–5, revealed a significant *diet x age Interaction ($F_{[2, 10]} = 8.40$, $p = 0.007$)*, with significant post hoc tests showing elevated CORT levels between adolescents and adults on *HFD ($p = 0.03$)* (Fig. 3B).

CRF1 Expression in ovaries and oocytes was not changed.

3.3.3. HPLC

One-way ANOVA (diet), n = 6 per group, revealed a significant difference in Dopamine in the Amygdala *($F_{[2,11]} = 4.42$, $p = 0.04$)*. Since the post hoc Test showed only significantly lower Dopamine levels

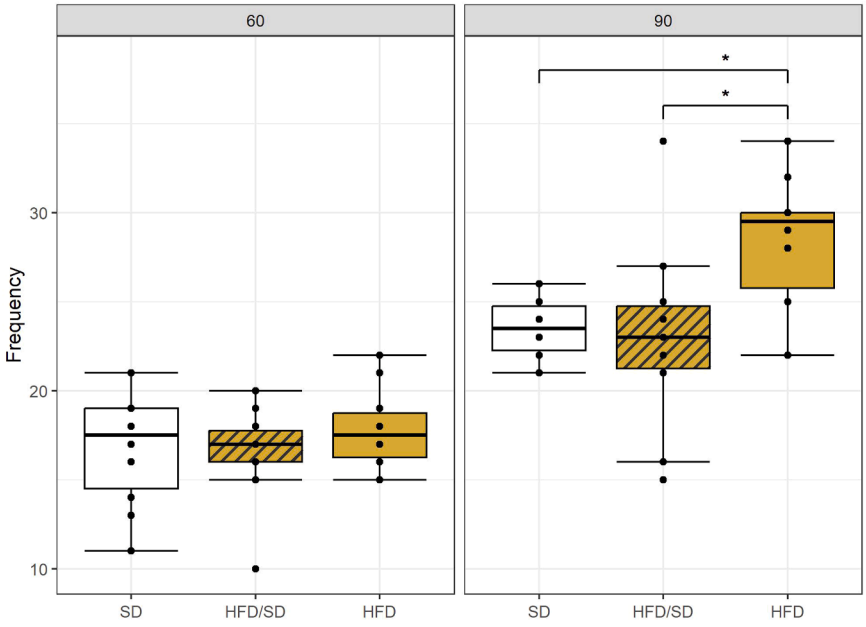

Fig. 2. Frequency of Entries into Closed Arms of EPM in F1. *Anxiety-related behavior was assessed using the EPM at PND 60 and PND 90 across diet groups (n = 10 per group). HFD-exposed groups entered the closed arms of the EPM more frequently in adulthood (PND 90), but not in adolescence (PND 60).* Statistical significance was determined by One-way ANOVA with Tukey's post hoc test (*p < 0.05). Boxplots display medians and interquartile ranges; whiskers extend to 1.5 × the IQR. Fill colors represent HFD exposure; striped patterns indicate a dietary switch.

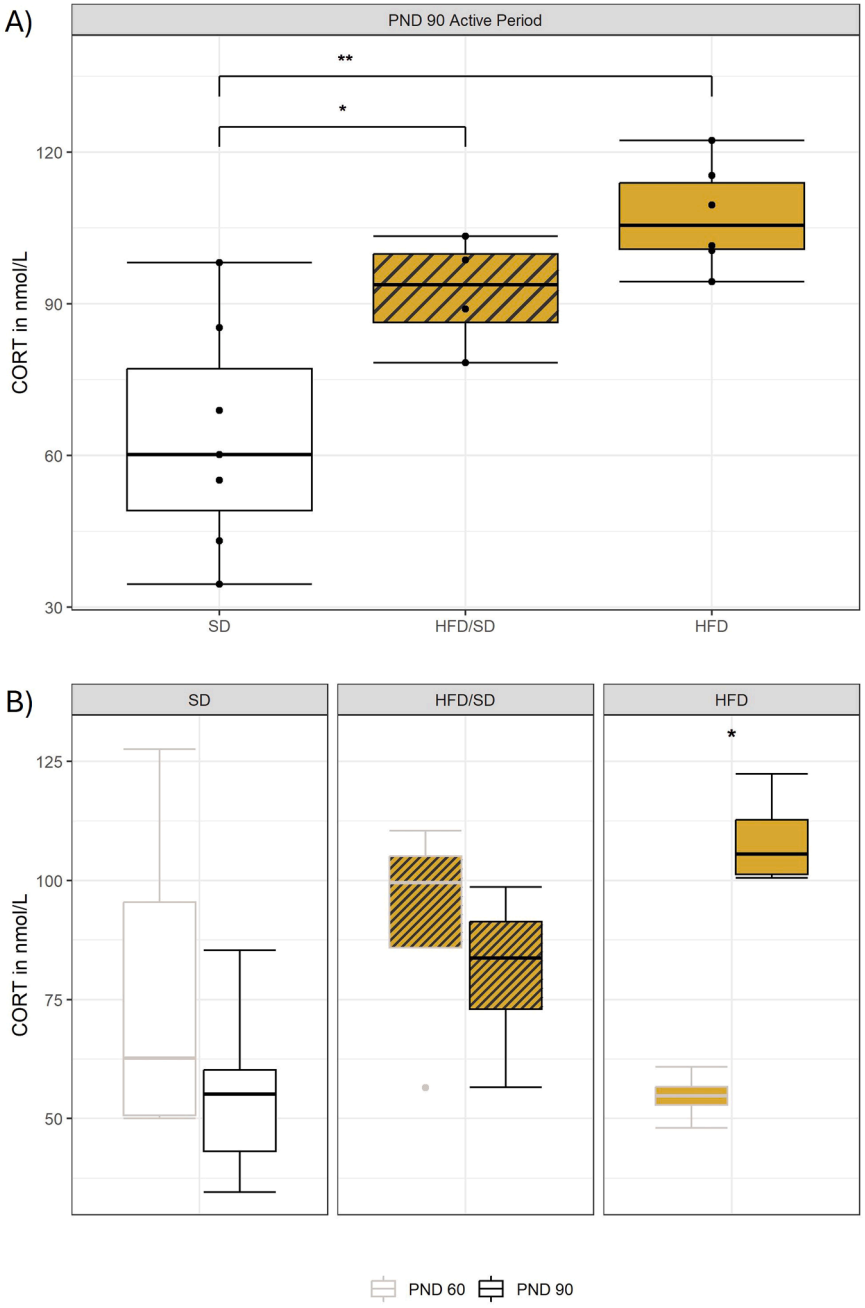

Fig. 3. HPA Axis. A) CORT Serum Levels During the Active Phase in Adulthood. At PND 90, CORT levels were significantly elevated in the HFD-exposed groups, despite the HFD/SD group having switched to SD by that time (n = 4–7 per group). Statistical significance was determined by One-way ANOVA with Tukey's post hoc test (*p < 0.05; **p < 0.01). **B) CORT Serum Levels Across Adolescence and Adulthood During the Active Phase.** In the HFD group only, CORT levels in adulthood (PND 90) were elevated compared to adolescence (PND 60) (n = 4–5 per group). Statistical significance was determined by Repeated measures ANOVA with Tukey's post hoc test (*p < 0.05). Boxplots show medians and interquartile ranges (IQR); whiskers extend to 1.5 × IQR. Fill colors indicate HFD exposure; striped patterns denote a dietary switch. Black outline represents PND 90, light outline represents PND60.

between *HFD* and *(HFD/SD) (p = 0.03)* and not between the SD and HFD groups, it cannot be concluded that diet had a significant impact on Dopamine in the Amygdala (see Supplementary Figure S3). All other neurotransmitters across all examined brain regions at PND 90 remained unchanged and were not significantly different (detailed values in Supplementary Table S1).

3.3.4. *Gut permeability*

Animals that were exposed to lifelong HFD showed a significantly increased gut permeability compared to SD or animals that switched from HFD to SD in adolescence, supported by an ANOVA (diet), n = 6, Levene's test p = 0.08 of the AUC revealing a *main effect for diet* ($F_{[2, 15]} = 6.22$, $p = 0.01$). As shown in Fig. 4 A/B, post hoc test showed significantly increased intestinal permeability of *HFD* compared *to HFD/SD (p = 0.02)* and *SD (p = 0.02)*.

3.3.5. *Microbiome*

Firmicutes and Bacteroidota were consistently the most abundant phyla observed across all diet groups and ages (Fig. 5A). Notably, groups sharing the same diet exhibited similar gut microbiome compositions. This pattern was further supported by differential abundance analysis. A strong similarity was found between HFD and HFD/SD, fed the same

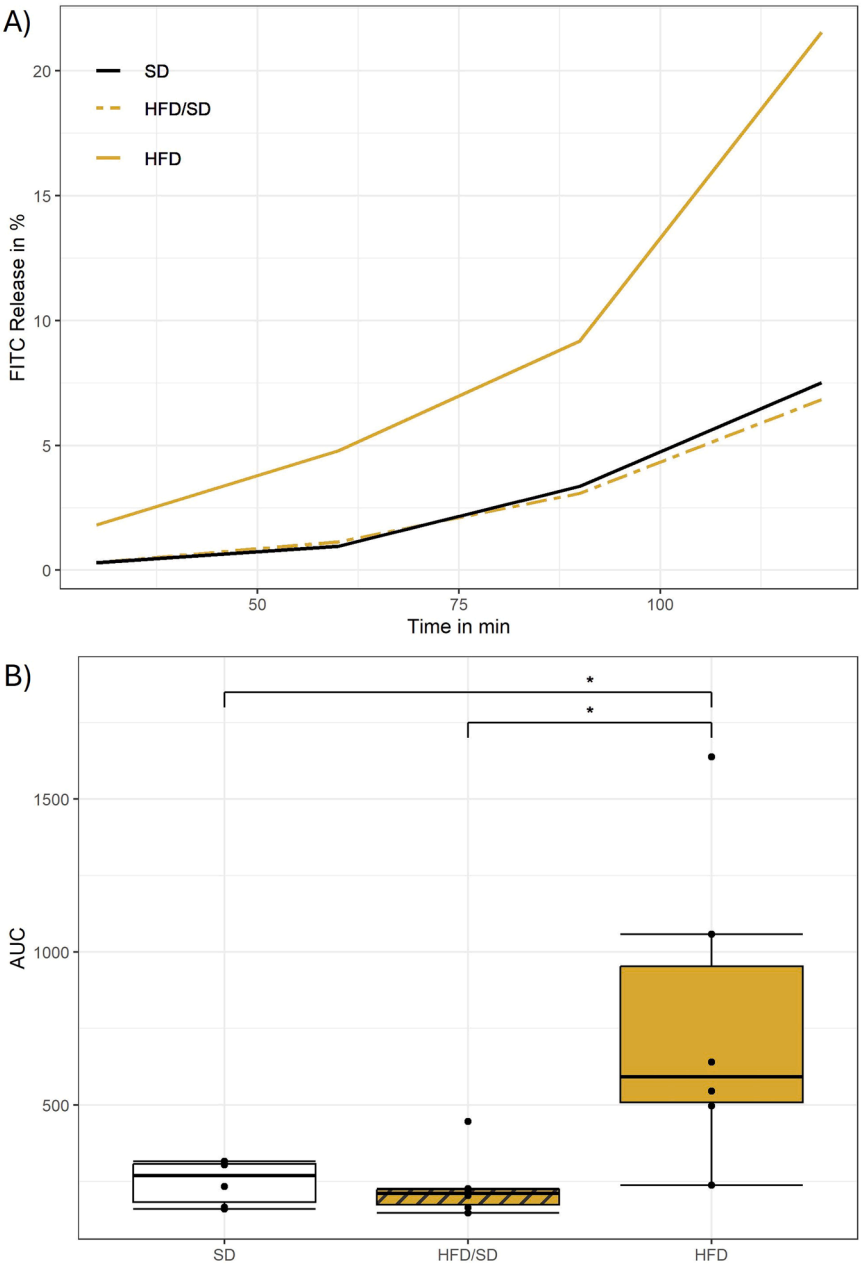

Fig. 4. Gut permeability. ***A)*** *Line graph showing the percentage of FITC release relative to maximum release over 2 h, and* ***B)*** the corresponding area under the curve (AUC) values at PND 90. The HFD group exhibited a significantly higher AUC of FITC release compared to the SD groups, indicating increased gut permeability (n = 6 per group). Statistical significance was determined by one-way ANOVA followed by Tukey's post hoc test (*p < 0.05). Boxplots represent medians and interquartile ranges (IQR); whiskers extend to 1.5 × IQR. Fill colors indicate HFD exposure, and striped patterns denote a dietary switch.

diet, at PND 60. In contrast to these groups, SD displayed significant differences at the phylum level, characterized by increased abundances of Bacteroidota, Actinobacteriota, and Proteobacteria, and decreased levels of Desulfobacterota, Firmicutes, and Verrucomicrobiota (Fig. 5B1; detailed values in Supplementary Table S2). These effects were partially reversed by PND 90 (Fig. 5B2; detailed values in Supplementary Table S3). Following one month on SD, HFD/SD exhibited microbial composition that more closely resembled that of SD. Specifically, Desulfobacterota, Firmicutes, and Verrucomicrobiota were significantly reduced in HFD/SD compared to HFD, consistent with the differences observed at PND 60. Interestingly, Actinobacteriota, which had been elevated in SD compared to HFD at PND 60, showed decreased levels at PND 90, although their abundance remained diet-dependent. A similar trend was observed for Bacteroidota. These findings suggest that the gut microbiome is influenced not only by diet but also by age-related dynamics (see Fig. 5B; detailed values in Supplementary Tables S3 and S4). However, the reversal was only partial, as the HFD/SD group's microbiome became more similar to that of the SD group, but showed generally smaller effect sizes (detailed values in Supplementary Table S4). Differences remained in the abundances of Firmicutes, Patescibacteria, and Bacteroidota between the HFD/SD and SD groups. Verrucomicrobiota was detected only in HFD-exposed animals and disappeared after the diet switch to SD in the HFD/SD group, suggesting this phylum is associated with HFD exposure.

Results of the genus-level differential abundance analysis using metadeconfoundR are provided in the Supplementary Data (Fig. S4 and S5, Table S5 and S6). Notably, a considerable proportion of taxa remained unclassified at the genus level and are therefore not

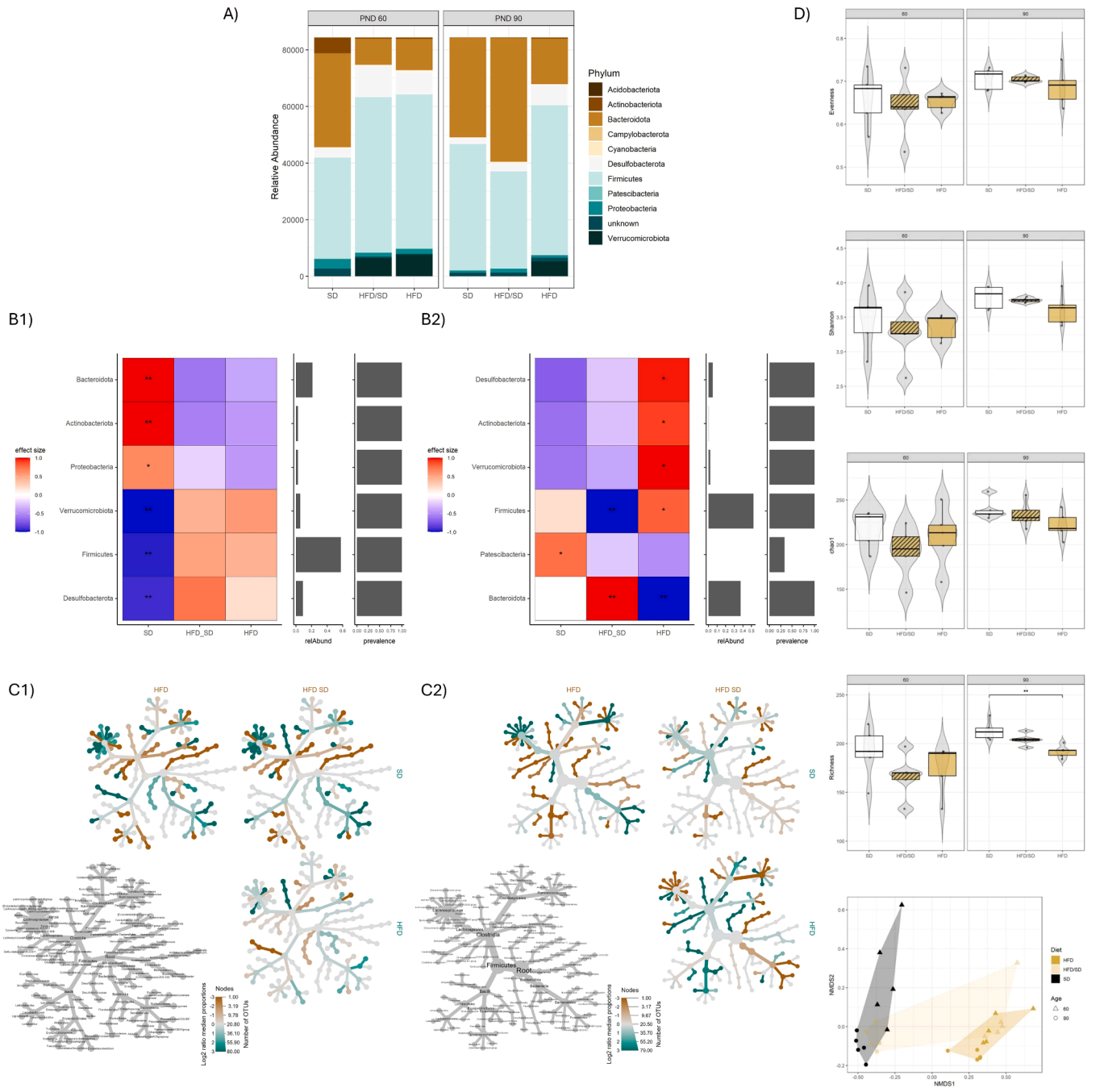

Fig. 5. Fecal Microbiome. A) Gut Microbiome Composition *at Phylum Level across diets at PND 60 (before diet switch in adolescence) and PND 90 (30 days after diet switch) in a stacked bar-plot.* **B) Differential Abundance of Phyla across Diets before (PND 60; B1) and after the Diet switch (PND 90; B2).** Heatmap displays Cliff's Delta effect sizes for differences in phylum-level abundance. Statistical significance was assessed using a two-sided Wilcoxon rank-sum test with FDR adjustment (* $p < 0.1$; $p < 0.001$). The left marginal bar plot shows the log-transformed relative abundance (relAbund) of each phylum. The right marginal bar plot shows proportion of samples containing each phylum (prevalence). Data are presented as mean ± SEM (n = 5). Detailed values are provided in the Supplementary Information. **C) Heat tree comparing diets of Genus before (PND 60; C1) and after the Diet switch (PND 90; C2).** Not classified Taxa are not presented. Gray reference tree (lower left) serves as a legend. Taxon colors indicate log2 fold changes in median read proportions between diet groups (n = 5 per group). Only significant differences (Wilcoxon rank-sum test with FDR correction) are shown. Green marks taxa enriched diet group shown in the row; brown indicates enrichment in the diet group shown in the column. **D) Diversity indices**. Alpha diversity indices (D1–4) and NMDS Visualization of Bray-Curtis Dissimilarity (D5). * $p < 0.05$.

represented in Figs. 5C1 and 5C2. At PND 60, the SD group showed increased abundances of several genera, including *Bifidobacterium, Butyricicoccus, Ligilactobacillus,* and *Tyzzerella*. In contrast, genera such as *Akkermansia, Epulopiscium, Holdemania*, and *Enterococcus* were significantly decreased compared to the HFD and HFD/SD groups. At PND 90, some of these patterns persisted. In SD, *Tyzzerella* remained elevated, while *Holdemania* remained decreased, despite both belonging to the same phylum (Firmicutes), illustrating divergent responses within the phylum. Interestingly, these significant changes were not observed in the HFD/SD group, indicating that, despite being switched to the same diet as the SD group for 30 days, the microbiota composition of the HFD/SD group did not fully align with that of the SD group. Notably, genera that were reduced in SD at PND 60, such as *Holdemania, Enterococcus, Akkermansia,* and *Epulopiscium*, were increased in the HFD

group at PND 90.

Alpha-diversity on operational taxonomic units (OTU) level was significantly influenced by age across all measured indices, with adult animals exhibiting higher diversity (Fig. 5D). Specifically, evenness was age-dependent ($F_{[1,\ 24]} = 8.43,\ p = 0.008$), as was the Shannon index ($F_{[1,\ 24]} = 10.60,\ p = 0.003$), the Chao1 index ($F_{(1,\ 12.13)} = 11.94,\ p = 0.005$), and Richness ($F_{(1,\ 12.10)} = 17.04,\ p = 0.001$). When analyzing Richness at PND 90 separately, a significant *diet main effect* was observed ($F_{[2,\ 12]} = 10.00,\ p = 0.003$; *Levene's Test 0.6*), with animals on the *HFD* showing significantly lower richness compared to those on the SD ($p = 0.002$) (Fig 5D4). **Bray-Curtis Dissimilarity** Analysis on OTU level showed significant main effects of *diet* ($F_{[2,\ 29]} = 9.18,\ R^2 = 0.290,\ p = 0.001$) and *age* ($F_{[1,\ 29]} = 11.32,\ R^2 = 0.179,\ p = 0.001$) as well as an *age x diet interaction* ($F_{[2,\ 29]} = 4.14,\ R^2 = 0.131,\ p = 0.003$). Subject ID was included in the model to approximate a repeated-measures design; however, it was not statistically significant. Residual variation accounted for $R^2 = 0.174$ of the total variance. Since beta dispersion analysis indicated significant heterogeneity for diet ($p = 0.02$), an Analysis of Similarities (ANOSIM) test was conducted, as it is less sensitive to differences in dispersion. The ANOSIM confirmed significant, moderate separation between dietary groups ($R = 0.4$, $p = 0.002$). Pairwise comparisons were performed for each time point to address significant age-related differences. At PND 60, no differences between *HFD* and *HFD/SD* were detected when both groups were on the same diet (Fig. 5D). However, significant differences were observed between *SD* compared to *HFD* ($p = 0.03$) and *HFD/SD* ($p = 0.04$). At PND 90, *SD* remained significantly different from *HFD* ($p = 0.03$). Following the diet switch from *HFD/SD* to *SD*, a significant difference emerged between *HFD/SD* and *HFD* ($p = 0.03$). Although NMDS visualization revealed a shift of *HFD/SD* towards *SD*, the groups remained significantly distinct ($p = 0.04$) (Fig. 5D5).

4. Discussion

This study sought to explore the effects of HFD exposure during adolescence and adulthood on females. The impact of HFD was most evident in the intestinal permeability and microbiome analysis, which demonstrated partial reversibility. In addition to diet-related changes, our findings highlight that age, independent of dietary factors, plays a critical role in shaping behavioral and metabolic outcomes. We found significant age differences in behavioral tests and several lipid metabolism markers, suggesting that cognition and metabolism are subjected to a developmental course. This study also demonstrates that the microbiome is shaped by diet and adapts dynamically to dietary changes, partially reversing the effects of previous diets. Behavioral analysis revealed some unexpected outcomes that may contribute to understanding sex differences since established literature focused primarily on male subjects. To the best of our knowledge, this is the first study looking into the role of high-fat nutrition on the HPA axis in oocytes and ovaries. Although this finding aligns with existing literature, the HPA axis was impaired systematically, with altered CORT serum levels; however, CRF1 expression in oocytes and ovaries did not differ significantly among the groups. The results suggest that this component of the HPA axis may not be responsible for the impairments observed in the offspring of mothers exposed to HFD, as described in the literature.

4.1. Weight

Interestingly, at PND 58 and prior to the dietary change, there were no differences in body weight between the SD and HFD groups. Nonetheless, following the diet switch from HFD to SD, animals gained significantly more weight than the other groups. This may appear counterintuitive at first, considering studies that indicate a preference for HFD over SD (Mazzone et al., 2020). However, it has been suggested that compensational overeating serves homeostatic purposes in specific states, such as fasting or exposure to an imbalanced diet (Minokoshi et al., 2020). Interestingly, corticotropin-releasing hormone (CRH) neurons, another player in the HPA axis (Minokoshi et al., 2020), regulate these processes. Additionally, Chan et al. found similar results, noting a peak in weight following a diet switch in mice and suggested that this is possibly due to the modulation of genes regulating fatty acid oxidation, which were found to be initially upregulated after prolonged exposure to HFD. This adaptation mechanism was disrupted, leading to gene downregulation (Chan et al., 2008). However, this effect decreased over time, with only animals exposed to HFD displaying significantly increased weight compared to the other groups. Although statistically, there was no significant difference at PND 90, the data still indicate that the HFD/SD group had an elevated body weight compared to the SD group, implying that weight loss, even after a diet switch in adolescence, may not be entirely reversible, which aligns with existing literature (Braga et al., 2021).

4.2. Behavior

Consistent with other findings, animals exposed to HFD throughout their entire lifespan displayed heightened anxious behavior in EPM compared to the other groups by entering the closed arm more often, while overall locomotor activity, measured as total distance moved, remained unaltered across the groups (Ziemens et al., 2022). Notably, exposure to HFD exclusively during adolescence did not induce abnormalities in EPM. This leads to the assumption that a longer exposition of HFD is needed to induce behavioral changes. Furthermore, EPM performance appears to be strongly influenced by age. Regardless of their diet, adult animals spent less time in closed arms but entered them more frequently than their younger counterparts. It can be concluded that this behavior is more representative of increased exploratory activity than of elevated anxiety.

The impact of age on behavior, consistent with existing literature, was also observed in PPI performance (Hadar et al., 2015). Older animals demonstrated increased pre-pulse inhibition, indicating ongoing sensorimotor gating development until PND90 (Hadar et al., 2015). Neither HFD exposure during adolescence nor exposure until adulthood impaired sensorimotor gating functioning. This contrasts with a previous study demonstrating sensorimotor gating impairments in male mice exposed to HFD during adolescence (Labouesse et al., 2013). Beyond species differences, the observed contradictions may be attributed to sex-specific responses to dietary regimes, suggesting males are more susceptible to dietary changes. The same rationale may be applied to the absence of cognitive impairments in NOR and T-Maze test, opposing reports of HFD-inducing alterations in these assessments both in adolescence and adulthood (Ziemens et al., 2022). Notably, the majority of studies referenced in the cited review involve male mice, underlying a longstanding necessity for pre-clinical studies focusing on female animals. We therefore speculate that this is not a discrepancy but rather due to sex differences in sensitivity and, consequently, response to HFD (Lloyd and Reyes, 2022; Deal et al., 2022). Limited research suggests that sex-specific hormonal mechanisms may underlie the differing behavioral outcomes in HFD-exposed rodents, including heightened stress responses in males and protective effects of estrogen in females (Acharya et al., 2023; Soulis et al., 2007).

Although there is evidence that neurotransmitters are affected by HFD exposure (da Silva et al., 2021), we were not able to replicate these results.

4.3. Gut

Aligning with findings from current literature that describes guts' architectural changes following HFD (Cordeiro et al., 2023; Rohr et al., 2020), gut permeability was significantly increased in lifelong HFD-exposed animals compared to animals that switched to a standard diet in adolescence, suggesting that HFD solely during adolescence may not induce permeability changes or may be reversible, further gut

permeability tests at adolescence before the diet switch are needed to confirm one of the hypotheses. However, when considered alongside microbiome data collected before and after the diet switch, the effects of HFD on gut permeability appear largely reversible. While adolescent HFD exposure resulted in alterations to the microbiome, it became closely comparable to lifelong SD following the diet switch.

Again, age is a critical factor, with fecal microbiome development paralleling brain development as a process that extends into adulthood, thereby extending the brain-gut axis theory (Mancabelli et al., 2024; Dash et al., 2022). In adults, microbial alpha diversity was generally higher. Interestingly, only richness showed significant decrease in adults exposed to lifelong HFD, indicating that prolonged exposure is necessary to impact alpha diversity. Other indices, such as the Shannon and Chao indices, remained unaffected, likely because there were no changes in evenness. The Beta Diversity of the microbiome in HFD-exposed animals during adolescence differed significantly from that of SD at the same age. However, in adulthood, the microbiome of those who transitioned to SD closely resembled that of the SD. This finding suggests that the effects of HFD on the microbiome are partially reversible and reflect a dynamic, adaptable process. This effect is also evident in the analysis of individual phyla: after switching to SD, the microbial composition of the HFD/SD group became similar to that of the SD group, leaving certain phyla uniquely associated with HFD exposure.

Consistent with the literature, we observed an increase in Firmicutes and a concurrent decrease in Bacteroidota during HFD exposure (Turnbaugh et al., 2008; Hildebrandt et al., 2009; Murphy et al., 2010). In addition to Firmicutes, the abundance of Actinobacteriota increased only at 90 days, and that of Desulfobacterota also increased with HFD exposure. These changes have been shown to be correlated with elevated proinflammatory cytokine expression, explaining the increased inflammation markers observed in obesity (Kim et al., 2019). Furthermore, Actinobacteriota are known to be associated with mucin degradation (Kim et al., 2019), and the increased abundance of this phylum may help explain the gut permeability impairments observed with HFD. Similarly, the increase in Desulfobacterota, which is linked to gut inflammation (Figliuolo et al., 2017), may also contribute to these effects. The restoration of certain phyla toward a composition resembling the SD microbiome is particularly noteworthy, especially with regard to Verrucomicrobiota, which was exclusively found in HFD-fed animals. After switching to SD at PND 60, no detectable Verrucomicrobiota was present at PND 90 in the HFD/SD group. Notably, at PND 90, certain taxa were significantly altered only in the SD group, but not in the HFD/SD group, indicating that, despite 30 days on the same diet as the SD group, the microbiota composition of the HFD/SD group did not completely converge with that of the SD group. On genus level, SD was associated with Taxa that are widely considered beneficial, including *Bifidobacterium, Butyricicoccus, and Ligilactobacillus*, as they have immunomodulatory effects, are involved in homeostasis, and contribute to intestinal barrier integrity (Gavzy et al., 2023; Siddiqui and Cresci, 2021; Indo et al., 2021). Surprisingly, *Tyzzerella* was also increased in SD, although frequently associated with HFD (Xu et al., 2022; Yang et al., 2025). Conversely, genera such as *Akkermansia, Holdemania*, and *Enterococcus* were significantly reduced in the SD. While *Akkermansia* is often associated with metabolic benefits, it has also been implicated in compromising mucin layer integrity and worsening disease in specific contexts (Chiantera et al., 2023). Similarly, *Holdemania* has been linked to negative metabolic profiles (Lippert et al., 2017). By PND 90, these genera, initially decreased in SD, showed increased abundance in HFD. The elevated presence of *Enterococcus* under HFD conditions is consistent with earlier findings, highlighting its association with diet-induced dysbiosis (Wei et al., 2024).

4.4. HPA axis

Alterations of HPA axis after HFD exposure are well-documented. However, these do not extend to the reproductive system, where neither the ovaries nor the oocytes showed a significant alteration in CRF1 expression. Aligning with the results from the EPM, where HFD animals exhibited more anxious behavior in adulthood, the CORT levels of HFD animals were elevated during that period, suggesting that HFD exposure time plays a key role in altering the HPA axis, as changes were not visible in adolescence. Dietary factors, such as HFD, strongly influence CORT, a key component of the HPA axis, by inducing inflammatory stimulation and, thus, HPA axis activation (Witchel and DeFranco, 2006). Although HPA axis is highly influenced by sex, studies associating CORT and HFD are scarce and mainly include male mice (Lizarbe et al., 2018). Our CORT level analysis indicates that the HPA axis of HFD-exposed female animals is compromised even after switching to SD in adolescence, as they exhibit higher CORT values during their active phase. Interestingly, our findings show that HFD exposure restricted to adolescence (HFD/SD) produces long-lasting HPA-axis alterations, without producing measurable changes in anxiety-like behavior in these animals. This suggests that transient adolescent HFD is insufficient to surpass the threshold needed to alter anxiety-like behavior. Instead, it appears to leave a persistent endocrine signature without producing measurable behavioral consequences, consistent with previous reports (Hryhorczuk et al., 2017). This dissociation implies that endocrine and behavioral systems can diverge and that corticosterone elevation alone does not reliably predict anxiety-like behavior (Mendes-Gomes et al., 2011; Sapolsky et al., 2000; MacDougall-Shackleton et al., 2019).

In contrast to males, females do not exhibit a difference in CORT levels from adolescence to adulthood (Laviola et al., 2002). HFD/SD animals displayed slightly lower, though not statistically significant, CORT levels compared to the HFD group and showed no age-related increase. We interpret this pattern as a modest attenuation of the HFD effect rather than evidence for a reversal of HPA-axis alterations.

Zaidan et al. demonstrated that maternal stress can be transmitted to the next generation by examining not only their offspring but also maternal oocytes and ovaries, which showed increased levels of CRF1, a receptor commonly used to assess the HPA axis (Zaidan et al., 2013; Zaidan and Gaisler-Salomon, 2015). To the best of our knowledge, this study is the first to examine the HPA axis within the reproductive system of females subjected to an HFD. The analysis of CRF1 expression in ovaries and oocytes did not reveal any differences between the groups, suggesting that the diet during the examined development period may not impact future generations with respect to the examined marker.

4.5. Serum

Consistent with previous reports, Triglyceride were not altered by age or diet (Spitler et al., 2025). This study further found that lipid and glucose metabolism change over the course of development. Most examined markers (except for triglyceride and cholesterol) decreased from adolescence to adulthood, irrespective of diet. Similar trajectories have been observed in longitudinal studies of pre-adolescents to young adults, suggesting that adaptive endocrinological processes during maturation exert a stronger influence than diet (Schienkiewitz et al., 2019; Mäkinen et al., 2025). Interestingly, sex differences in fat metabolism have also been reported, indicating a connection between aging, sexual maturation, and metabolic parameters. Further studies are warranted to elucidate the mechanisms underlying these observations.

As described previously, the exposure duration significantly influences the extent of alterations in fat metabolism (Rodríguez-Correa et al., 2020). HFD solely during adolescence was not sufficient to introduce changes. The extended exposure until adulthood alone led to elevated cholesterol and LDL levels, potentially due to the regulation of fatty acid oxidation genes associated with the duration of HFD (Chan et al., 2008). Elevated levels of cholesterol and LDL are associated with an increased risk of atherosclerotic cardiovascular disease, a leading cause of mortality (Barquera et al., 2015). Interestingly, in HFD-exposed animals, increased *Heldomania* abundance at PND 90 was accompanied by elevated LDL levels, a genus previously implicated in negative

regulation of lipid metabolism (Lippert et al., 2017). In contrast, in SD-exposed animals, higher *Bifidobacterium* abundance was accompanied with unchanged LDL, consistent with its well-known cholesterol-lowering effects mediated through bile salt hydrolase activity (Zanotti et al., 2015; Liu et al., 2025). These findings suggest that diet-driven shifts in microbial taxa can potentially influence metabolic outcomes.

It becomes evident that the exposure duration of HFD determines the degree of altered metabolism and behavior. Our study showed that HFD had an irreversible impact on the HPA axis solely during adolescence. However, only behavioral and lipid metabolic changes were observed in animals with lifelong HFD. Other studies have reported that diet switch from HFD in midlife is beneficial for metabolism and behavior (Braga et al., 2021), indicating that adverse effects following HFD could be rescued upon an early-life switch with shorter HFD exposure.

4.6. Limitations

Notably, the found disruption of lipid metabolism is linked to an increased risk for cardiovascular diseases, although cardiovascular events tend to occur later in life (Lu et al., 2015). This study was limited to a brief observation period, specifically until reaching adulthood. Given the context of an increasingly aging and unhealthy society (Jura and Kozak, 2016), it is necessary for future studies to incorporate an extended observation period to examine dietary effects in older, respectively, geriatric subjects.

5. Conclusion

This study highlights the long-term adverse effects of HFD on female behavior, the HPA axis, and gut health, with some effects being reversible through dietary changes in adolescence.

However, given the unaltered CRF1 expression in oocytes of HFD-exposed females, its involvement in the reported adverse outcomes in offspring of HFD-exposed dams appears limited, highlighting the need to explore alternative mechanisms. Epigenetic modifications and a more detailed investigation of the HPA axis may provide insights into these effects. Given the substantial alterations in the female microbiome dynamically changing to diet, this study adds to growing evidence of microbiome's role as a possible transmission route in maternal HFD-induced changes in their offspring.

Author statement

All author contributions have been detailed in the CRediT taxonomy upon manuscript submission.

CRediT authorship contribution statement

Christine Winter: Writing – review & editing, Supervision, Funding acquisition, Data curation. **Ravit Hadar:** Writing – review & editing, Supervision, Methodology, Funding acquisition, Data curation, Conceptualization. **Till Birkner:** Writing – review & editing, Software, Methodology. **Elena Popova:** Writing – review & editing, Methodology. **Gül Asude:** Writing – review & editing, Methodology, Investigation. **Ulrike Löber:** Writing – review & editing, Methodology. **Alexandra Ott:** Writing – original draft, Visualization, Methodology, Investigation, Formal analysis.

Declaration of Competing Interest

The authors declare that they have no known competing financial interests or personal relationships that could have appeared to influence the work reported in this paper.

Acknowledges

Open Access funding enabled and organized by Projekt DEAL.

Synlab.vet analyzed serum samples regarding lipid and sugar metabolism. DNA extraction and 16S rDNA sequencing of stool samples were performed in the Microbiome Laboratory of the Institut für Klinische Molekularbiologie (IKMB). Microbiome sequencing received infrastructure support from the DFG Excellence Cluster 2167 "Precision Medicine in Chronic Inflammation" (PMI) and the DFG Research Unit 5042 „miTarget". This study was further supported by TRR 265, WI 2140/5–1, and HA 8469/2–1.

Appendix A. Supporting information

Supplementary data associated with this article can be found in the online version at doi:10.1016/j.brainresbull.2026.111883.

References

Acharya, K.D., Graham, M., Raman, H., Parakoyi, A.E.R., Corcoran, A., Belete, M., et al., 2023. Estradiol-mediated protection against high-fat diet induced anxiety and obesity is associated with changes in the gut microbiota in female mice. Sci. Rep. 13 (1), 4776.

Antunes, M., Biala, G., 2012. The novel object recognition memory: neurobiology, test procedure, and its modifications. Cogn. Process. 13 (2), 93–110.

Barnard, N.D., Bunner, A.E., Agarwal, U., 2014. Saturated and trans fats and dementia: a systematic review. Neurobiol. Aging 35 (2), S65–S73.

Barquera, S., Pedroza-Tobías, A., Medina, C., Hernández-Barrera, L., Bibbins-Domingo, K., Lozano, R., et al., 2015. Global overview of the epidemiology of atherosclerotic cardiovascular disease. Arch. Med. Res. 46 (5), 328–338.

Bates, D., Bolker, Maechler M., Walker, B., 2015. S. Fitting linear mixed-effects models using lme4. J. Stat. Softw. 67 (1), 1–48.

Bedarf, J.R., Beraza, N., Khazneh, H., Özkurt, E., Baker, D., Borger, V., et al., 2021. Much ado about nothing? Off-target amplification can lead to false-positive bacterial brain microbiome detection in healthy and Parkinson's disease individuals. Microbiome 9 (1), 75.

Birkner, T., 2024. metadeconfoundR: covariate-sensitive analysis of cross-sectional high-dimensional data. R. Package Version 1. 0. 2.

Boitard, C., Parkes, S.L., Cavaroc, A., Tantot, F., Castanon, N., Layé, S., et al., 2016. Switching adolescent high-fat diet to adult control diet restores neurocognitive alterations. Front. Behav. Neurosci. 10, 225.

Braga, S.P., Delanogare, E., Machado, A.E., Prediger, R.D., Moreira, E.L.G., 2021. Switching from high-fat feeding (HFD) to regular diet improves metabolic and behavioral impairments in middle-aged female mice. Behav. brain Res. 398, 112969.

Buckley, J., 2018. Availability of high-fat foods might drive the obesity epidemic. Nat. Rev. Endocrinol. 14 (10), 574–575.

Buffington, S.A., Di Prisco, G.V., Auchtung, T.A., Ajami, N.J., Petrosino, J.F., Costa-Mattioli, M., 2016. Microbial reconstitution reverses maternal diet-induced social and synaptic deficits in offspring. Cell 165 (7), 1762–1775.

Chan M.Y., Zhao Y., Heng C.K.J.O. Sequential responses to high-fat and high-calorie feeding in an obese mouse model. 2008;16(5):972–978.

Chiantera, V., Laganà, A.S., Basciani, S., Nordio, M., Bizzarri, M., 2023. A Critical perspective on the supplementation of akkermansia muciniphila: benefits and harms. Life [Internet] 13 (6).

Choi, J.K., He, X., 2013. vitro maturation of cumulus-oocyte complexes for efficient isolation of oocytes from outbred deer mice. PloS One 8 (2), e56158.

Cifre, M., Palou, A., Oliver, P., 2018. Cognitive impairment in metabolically-obese, normal-weight rats: identification of early biomarkers in peripheral blood mononuclear cells. Mol. Neurodegener. 13 (1), 14.

Cordeiro, G.S., Góis, M.B., Santos, L.S., Espírito-Santo, D.A., Silva, R.T., Pereira, M.U., et al., 2023. Perinatal and post-weaning exposure to a high-fat diet causes histomorphometric, neuroplastic, and histopathological changes in the rat ileum. J. Dev. Orig. Health Dis. 14 (2), 231–241.

Dash, S., Syed, Y.A., Khan, M.R., 2022. Understanding the role of the gut microbiome in brain development and its association with neurodevelopmental psychiatric disorders. Front. Cell Dev. Biol. 10, 880544.

Deacon, R.M.J., Rawlins, J.N.P., 2006. T-maze alternation in the rodent. Nat. Protoc. 1 (1), 7–12.

Deal, A.W., Thurman, A., Seshie, O., Szalanczy, A., Beeson, A., Cockerham, M., et al., 2022. Sex and genetic specific effects on behavioral, but not metabolic, responses to a high fat diet in heterogeneous stock rats. bioRxiv 2022. .03.25.485743.

Edgar, R.C., 2013. UPARSE: highly accurate OTU sequences from microbial amplicon reads. Nat. Methods 10 (10), 996–998.

Edwards, L.M., Murray, A.J., Holloway, C.J., Carter, E.E., Kemp, G.J., Codreanu, I., et al., 2011. Short-term consumption of a high-fat diet impairs whole-body efficiency and cognitive function in sedentary men. FASEB J. Off. Publ. Fed. Am. Soc. Exp. Biol. 25 (3), 1088–1096.

Ennaceur, A., Delacour, J., 1988. A new one-trial test for neurobiological studies of memory in rats. 1: behavioral data. Behav. brain Res. 31 (1), 47–59.

Figliuolo, V.R., Dos Santos, L.M., Abalo, A., Nanini, H., Santos, A., Brittes, N.M., et al., 2017. Sulfate-reducing bacteria stimulate gut immune responses and contribute to inflammation in experimental colitis. Life Sci. 189, 29–38.
Forslund, S.K., Chakaroun, R., Zimmermann-Kogadeeva, M., Markó, L., Aron-Wisnewsky, J., Nielsen, T., et al., 2021. Combinatorial, additive and dose-dependent drug–microbiome associations. Nature 600 (7889), 500–505.
Foster, Z.S., Sharpton, T.J., Grünwald, N.J., 2017. Metacoder: an R package for visualization and manipulation of community taxonomic diversity data. PLoS Comput. Biol. 13 (2), e1005404.
Gavzy, S.J., Kensiski, A., Lee, Z.L., Mongodin, E.F., Ma, B., Bromberg, J.S., 2023. Bifidobacterium mechanisms of immune modulation and tolerance. Gut Microbes 15 (2), 2291164.
Godfrey, K.M., Reynolds, R.M., Prescott, S.L., Nyirenda, M., Jaddoe, V.W., Eriksson, J.G., et al., 2017. Influence of maternal obesity on the long-term health of offspring. Lancet Diabetes & Endocrinol. 5 (1), 53–64.
Hadar, R., Soto-Montenegro, M.L., Götz, T., Wieske, F., Sohr, R., Desco, M., et al., 2015. Using a maternal immune stimulation model of schizophrenia to study behavioral and neurobiological alterations over the developmental course. Schizophr. Res. 166 (1-3), 238–247.
Harmancıoğlu, B., Kabaran, S., 2023. Maternal high fat diets: impacts on offspring obesity and epigenetic hypothalamic programming. Front. Genet. 14, 1158089.
Hauswedell, H., Singer, J., Reinert, K., 2014. Lambda: the local aligner for massive biological data. Bioinforma. (Oxf. Engl.) 30 (17), i349–i355.
Hildebrandt, M.A., Hoffmann, C., Sherrill–Mix, S.A., Keilbaugh, S.A., Hamady, M., Chen, Y.Y., et al., 2009. High-fat diet determines the composition of the murine gut microbiome independently of obesity. Gastroenterology 137 (5), 1716–1724 e2.
Holloway, C.J., Cochlin, L.E., Emmanuel, Y., Murray, A., Codreanu, I., Edwards, L.M., et al., 2011. A high-fat diet impairs cardiac high-energy phosphate metabolism and cognitive function in healthy human subjects. Am. J. Clin. Nutr. 93 (4), 748–755.
Hryhorczuk, C., Décarie-Spain, L., Sharma, S., Daneault, C., Rosiers, C.D., Alquier, T., et al., 2017. Saturated high-fat feeding independent of obesity alters hypothalamus-pituitary-adrenal axis function but not anxiety-like behaviour. Psychoneuroendocrinology 83, 142–149.
Indo, Y., Kitahara, S., Tomokiyo, M., Araki, S., Islam, M.A., Binghui, Z., et al., 2021. Ligilactobacillus salivarius strains isolated from the porcine gut modulate innate immune responses in epithelial cells and improve protection against intestinal viral-bacterial superinfection. Front. Immunol. 12, 652923.
Jura, M., Kozak, L.P., 2016. Obesity and related consequences to ageing. Age (Dordr. Neth.) 38 (1), 23.
Kim, S.J., Kim, S.E., Kim, A.R., Kang, S., Park, M.Y., Sung, M.K., 2019. Dietary fat intake and age modulate the composition of the gut microbiota and colonic inflammation in C57BL/6J mice. BMC Microbiol. 19 (1), 193.
Kozich, J.J., Westcott, S.L., Baxter, N.T., Highlander, S.K., Schloss, P.D., 2013. Development of a dual-index sequencing strategy and curation pipeline for analyzing amplicon sequence data on the MiSeq Illumina sequencing platform. Appl. Environ. Microbiol. 79 (17), 5112–5120.
Kuznetsova, A., Brockhoff, P.B., Christensen, R.H.B., 2017. lmerTest package: tests in linear mixed effects models. J. Stat. Softw. 82 (13), 1–26.
Labouesse, M.A., Stadlbauer, U., Langhans, W., Meyer, U., 2013. Chronic high fat diet consumption impairs sensorimotor gating in mice. Psychoneuroendocrinology 38 (11), 2562–2574.
Lafortuna, C.L., Tovar, A.R., Rastelli, F., Tabozzi, S.A., Caramenti, M., Orozco-Ruiz, X., et al., 2017. Clinical, functional, behavioural and epigenomic biomarkers of obesity, 22 (10), 1655–1681.
Laviola, G., Adriani, W., Morley-Fletcher, S., Terranova, M., 2002. Peculiar response of adolescent mice to acute and chronic stress and to amphetamine: evidence of sex differences. Behav. brain Res. 130 (1), 117–125.
Lenth, R.V., 2024. emmeans: estimated marginal means, aka least-squares means. R. Package Version 1. 10. 6.
Leo, A., Citraro, R., Tallarico, M., Iannone, M., Fedosova, E., Nesci, V., et al., 2019. Cognitive impairment in the WAG/Rij rat absence model is secondary to absence seizures and depressive-like behavior. Prog. Neuro-Psychopharmacol. Biol. Psychiatry 94, 109652.
Li, H., 2018. Minimap2: pairwise alignment for nucleotide sequences. Bioinforma. (Oxf. Engl.) 34 (18), 3094–3100.
Lippai, R., Veres-Székely, A., Szikszi, E., Iwakura, Y., Pap, D., Rokonay, R., et al., 2021. Immunomodulatory role of Parkinson's disease 7 in inflammatory bowel disease. Sci. Rep. 11 (1), 14582.
Lippert, K., Kedenko, L., Antonielli, L., Kedenko, I., Gemeier, C., Leitner, M., et al., 2017. Gut microbiota dysbiosis associated with glucose metabolism disorders and the metabolic syndrome in older adults. Benef. Microbes 8 (4), 545–556.
Liu, Y., Kuang, W., Li, M., Wang, Z., Liu, Y., Zhao, M., et al., 2025. Cholesterol-lowering mechanism of lactobacillus bile salt hydrolase through regulation of bifidobacterium pseudolongum in the gut microbiota. Nutr. [Internet] 17 (18), 3019 p..
Livak, K.J., Schmittgen, T.D., 2001. Analysis of relative gene expression data using real-time quantitative PCR and the 2−ΔΔCT method. Methods 25 (4), 402–408.
Lizarbe, B., Soares, A.F., Larsson, S., Duarte, J.M.N., 2018. Neurochemical modifications in the hippocampus, cortex and hypothalamus of mice exposed to long-term high-fat diet. Front. Neurosci. 12, 985.
Lloyd, K., Reyes, T., 2022. High fat diet consumption restricted to adolescence has minimal effects on adult executive function that vary by sex. Nutr. Neurosci. 25 (4), 801–811.
Lu, L., Liu, M., Sun, R., Zheng, Y., Zhang, P., 2015. Myocardial Infarction: symptoms and Treatments. Cell Biochem. Biophys. 72 (3), 865–867.
Mabrok, H.B., Ramadan, A.A., Hamed, I.M., Mohamed, D.A., 2024. Obesity as inducer of cognitive function decline via dysbiosis of gut microbiota in rats. Brain Sci. 14 (8).
MacDougall-Shackleton, S.A., Bonier, F., Romero, L.M., Moore, I.T., 2019. Glucocorticoids and "stress" are not synonymous. Integr. Org. Biol. 1 (1), obz017.
Mäkinen, V.P., Kähönen, M., Lehtimäki, T., Hutri, N., Rönnemaa, T., Viikari, J., et al., 2025. Metabolic transition from childhood to adulthood based on two decades of biochemical time series in three longitudinal cohorts. Int. J. Epidemiol. 54 (2).
Mancabelli, L., Milani, C., De Biase, R., Bocchio, F., Fontana, F., Lugli, Gabriele A., et al., 2024. Taxonomic and metabolic development of the human gut microbiome across life stages: a worldwide metagenomic investigation. mSystems 9 (4), e01294–23.
Martinez Arbizu P. pairwiseAdonis: Pairwise Multilevel Comparison using Adonis. R package version 0.4.1, commit cb190f7668a0c82c0b0853927db239e7b9ec3e83; 2017.
Mateer, S.W., Cardona, J., Marks, E., Goggin, B.J., Hua, S., Keely, S., 2016. Ex vivo intestinal sacs to assess mucosal permeability in models of gastrointestinal disease. J. Vis. Exp. (108), e53250-e.
Mattei, D., Djodari-Irani, A., Hadar, R., Pelz, A., de Cossío, L.F., Goetz, T., et al., 2014. Minocycline rescues decrease in neurogenesis, increase in microglia cytokines and deficits in sensorimotor gating in an animal model of schizophrenia. Brain Behav. Immun. 38, 175–184.
Mazzone, C.M., Liang-Guallpa, J., Li, C., Wolcott, N.S., Boone, M.H., Southern, M., et al., 2020. High-fat food biases hypothalamic and mesolimbic expression of consummatory drives. Nat. Neurosci. 23 (10), 1253–1266.
Mendes-Gomes, J., Miguel, T.T., Amaral, V.C., Nunes-de-Souza, R.L., 2011. Corticosterone does not change open elevated plus maze-induced antinociception in mice. Horm. Behav. 60 (4), 408–413.
Minokoshi, Y., Nakajima, K.I., Okamoto, S., 2020. Homeostatic versus hedonic control of carbohydrate selection. J. Physiol. 598 (18), 3831–3844.
Murphy, E.F., Cotter, P.D., Healy, S., Marques, T.M., O'Sullivan, O., Fouhy, F., et al., 2010. Composition and energy harvesting capacity of the gut microbiota: relationship to diet, obesity and time in mouse models. Gut 59 (12), 1635–1642.
de Noronha, S., de Moraes, L.A.G., Hassell Jr., J.E., Stamper, C.E., Arnold, M.R., Heinze, J.D., et al., 2024. High-fat diet, microbiome-gut-brain axis signaling, and anxiety-like behavior in male rats. Biol. Res. 57 (1), 23.
Obesity WHOCo, World Health Organization, Division of Noncommunicable D, World Health Organization, Programme of Nutrition, F., Reproductive, H., 1998. Obesity: preventing and managing the global epidemic: report of a WHO consultation on obesity, Geneva, 3-5 June 1997. World Health Organization, Geneva.
Oksanen, J., Simpson, G., Blanchet, F., Kindt, R., Legendre, P., Minchin, P., et al., 2025. Vegan community ecology package. R. Package Version 2. 7-1.
Ott, A., Ghirardello, O., Tanev, K., Altschüler, J., Gül, A.Z., Kruschke, Z., et al., 2025. Pre-reproductive excessive alcohol and maternal immune activation differentially affect offspring behavior, neurobiology, and brain volume in a sex-dependent manner. Prog. neuro-Psychopharmacol. & Biol. Psychiatry 143, 111550.
Özkurt, E., Fritscher, J., Soranzo, N., Ng, D.Y.K., Davey, R.P., Bahram, M., et al., 2022. LotuS2: an ultrafast and highly accurate tool for amplicon sequencing analysis. Microbiome 10 (1), 176.
Puente-Sánchez, F., Aguirre, J., Parro, V., 2016. A novel conceptual approach to read-filtering in high-throughput amplicon sequencing studies. Nucleic Acids Res. 44 (4), e40.
Pulungan, A.B., Puteri, H.A., Ratnasari, A.F., Hoey, H., Utari, A., Darendeliler, F., et al., 2024. Childhood obesity as a global problem: a cross-sectional survey on global awareness and national program implementation. J. Clin. Res. Pediatr. Endocrinol. 16 (1), 31–40.
Ratsika, A., Codagnone, M.G., Bastiaanssen, T.F.S., Hoffmann Sarda, F.A., Lynch, C.M.K., Ventura-Silva, A.P., et al., 2024. Maternal high-fat diet-induced microbiota changes are associated with alterations in embryonic brain metabolites and adolescent behaviour. Brain Behav. Immun. 121, 317–330.
Roberts, R.O., Roberts, L.A., Geda, Y.E., Cha, R.H., Pankratz, V.S., O'Connor, H.M., et al., 2012. Relative intake of macronutrients impacts risk of mild cognitive impairment or dementia. J. Alzheimer's. Dis. JAD 32 (2), 329–339.
Rodriguez, J.S., Rodríguez-González, G.L., Reyes-Castro, L.A., Ibáñez, C., Ramírez, A., Chavira, R., et al., 2012. Maternal obesity in the rat programs male offspring exploratory, learning and motivation behavior: prevention by dietary intervention pre-gestation or in gestation, 30 (2), 75–81.
Rodríguez-Correa, E., González-Pérez, I., Clavel-Pérez, P.I., Contreras-Vargas, Y., Carvajal, K., 2020. Biochemical and nutritional overview of diet-induced metabolic syndrome models in rats: what is the best choice? Nutr. & Diabetes 10 (1), 24.
Rognes, T., Flouri, T., Nichols, B., Quince, C., Mahé, F., 2016. VSEARCH: a versatile open source tool for metagenomics. PeerJ 4, e2584.
Rohr, M.W., Narasimhulu, C.A., Rudeski-Rohr, T.A., Parthasarathy, S., 2020. Negative effects of a high-fat diet on intestinal permeability: a review. Adv. Nutr. 11 (1), 77–91.
Saary, P., Forslund, K., Bork, P., Hildebrand, F., 2017. RTK: efficient rarefaction analysis of large datasets. Bioinforma. (Oxf. Engl.) 33 (16), 2594–2595.
Sapolsky, R.M., Romero, L.M., Munck, A.U., 2000. How do glucocorticoids influence stress responses? Integrating permissive, suppressive, stimulatory, and preparative actions. Endocr. Rev. 21 (1), 55–89.
Schienkiewitz, A., Truthmann, J., Ernert, A., Wiegand, S., Schwab, K.O., Scheidt-Nave, C., 2019. Age, maturation and serum lipid parameters: findings from the German health survey for children and adolescents. BMC Public Health 19 (1), 1627.
Schoeler, M., Ellero-Simatos, S., Birkner, T., Mayneris-Perxachs, J., Olsson, L., Brolin, H., et al., 2023. The interplay between dietary fatty acids and gut microbiota influences host metabolism and hepatic steatosis. Nat. Commun. 14 (1), 5329.
Shoubridge, A.P., Choo, J.M., Martin, A.M., Keating, D.J., Wong, M.L., Licinio, J., et al., 2022. The gut microbiome and mental health: advances in research and emerging priorities. Mol. Psychiatry 27 (4), 1908–1919.

Siddiqui, M.T., Cresci, G.A.M., 2021. The immunomodulatory functions of butyrate. J. Inflamm. Res. 14, 6025–6041.
da Silva, L.O., da Silva Aragão, R., Duarte Barros, M.D.L., Nogueira Ferraz-Pereira, K., Lins Pinheiro, I., Galindo, L.C.M., 2021. Maternal exposure to high-fat diet modifies anxiety-like/depression-like behaviors and compounds of Serotonergic System in offspring: A preclinical systematic review. International journal developmental neuroscience official journal International Society Developmental Neuroscience 81 (5), 371–385.
Soulis, G., Papalexi, E., Kittas, C., Kitraki, E., 2007. Early impact of a fat-enriched diet on behavioral responses of male and female rats. Behav. Neurosci. 121 (3), 483–490.
Spear, L.P., 2000. The adolescent brain and age-related behavioral manifestations. Neurosci. Biobehav. Rev. 24 (4), 417–463.
Spitler, K.M., Shetty, S.K., Davies, B.S.J., 2025. Effects of age and diet on triglyceride metabolism in mice. J. Lipid Res 66 (1), 100706.
Troci, A., Zimmermann, O., Esser, D., Krampitz, P., May, S., Franke, A., et al., 2022. B-cell-depletion reverses dysbiosis of the microbiome in multiple sclerosis patients. Sci. Rep. 12 (1), 3728.
Turnbaugh, P.J., Bäckhed, F., Fulton, L., Gordon, J.I., 2008. Diet-induced obesity is linked to marked but reversible alterations in the mouse distal gut microbiome. Cell host & Microbe 3 (4), 213–223.
Wei, C., Xu, T., Geng, Y., Yang, J., Lv, H., Guo, My, 2024. High-fat diet disrupts the gut microbiome, leading to inflammation, damage to tight junctions, and apoptosis and necrosis in Nyctereutes procyonoides intestines. Microbiol. Spectr. 12 (4), e0418223.
Wickham, H., Averick, M., Bryan, J., Chang, W., McGowan, L.D.A., François, R., et al., 2019. Welcome to the tidyverse. J. Open Source Softw. 4 (43), 1686.
Winter, C., Djodari-Irani, A., Sohr, R., Morgenstern, R., Feldon, J., Juckel, G., et al., 2009. Prenatal immune activation leads to multiple changes in basal neurotransmitter levels in the adult brain: implications for brain disorders of neurodevelopmental origin such as schizophrenia. Int. J. Neuropsychopharmacol. 12 (4), 513–524.
Witchel, S.F., DeFranco, D.B., 2006. Mechanisms of disease: regulation of glucocorticoid and receptor levels–impact on the metabolic syndrome. Nat. Clin. Pract. Endocrinol. & Metab. 2 (11), 621–631.
Xu, A.A., Kennedy, L.K., Hoffman, K., White, D.L., Kanwal, F., El-Serag, H.B., et al., 2022. Dietary fatty acid intake and the colonic gut microbiota in humans. Nutrients 14 (13).
Yang, Y., Zhan, J., Cheng, J., Cao, Y., Wu, C., 2025. Coptis chinensis shows distinct effects on hyperlipidemia and gut microbiota in high-fat diet induced mice with cold or hot syndrome. Chin. Herb. Med.
Yilmaz, P., Parfrey, L.W., Yarza, P., Gerken, J., Pruesse, E., Quast, C., et al., 2014. The SILVA and "All-species living tree project (LTP)" taxonomic frameworks. Nucleic Acids Res. 42 (Database), D643–D648.
Zaidan, H., Gaisler-Salomon, I., 2015. Prereproductive stress in adolescent female rats affects behavior and corticosterone levels in second-generation offspring. Psychoneuroendocrinology 58, 120–129.
Zaidan, H., Leshem, M., Gaisler-Salomon, I., 2013. Prereproductive stress to female rats alters corticotropin releasing factor type 1 expression in ova and behavior and brain corticotropin releasing factor type 1 expression in offspring. Biol. Psychiatry 74 (9), 680–687.
Zanotti, I., Turroni, F., Piemontese, A., Mancabelli, L., Milani, C., Viappiani, A., et al., 2015. Evidence for cholesterol-lowering activity by Bifidobacterium bifidum PRL2010 through gut microbiota modulation. Appl. Microbiol Biotechnol. 99 (16), 6813–6829.
Ziemens, D., Touma, C., Rappeneau, V., 2022. Neurobiological mechanisms modulating emotionality, cognition and reward-related behaviour in high-fat diet-fed rodents. Int. J. Mol. Sci. 23 (14).